Establishment of CHO cell lines expressing four *N*-methyl-D-aspartate receptor subtypes and characterization of a novel antagonist PPDC

Shigeo Uchino[a,*], Wakako Watanabe[b], Takeshi Nakamura[c], Satoshi Shuto[d], Yuji Kazuta[d], Akira Matsuda[d], Sadayo Nakajima-Iijima[b], Yoshihisa Kudo[c], Shinichi Kohsaka[a], Masayoshi Mishina[e]

[a] *Department of Neurochemistry, National Institute of Neuroscience, 4-1-1 Ogawahigashi, Kodaira, Tokyo 187-8502, Japan*
[b] *Pharmaceuticals Discovery Laboratory, Yokohama Research Center, Mitsubishi-Tokyo Pharmaceuticals Inc., 1000 Kamoshida, Aoba-ku, Yokohama 227-8502, Japan*
[c] *Department of Cellular Neurobiology, Tokyo University of Pharmacy and Life Sciences, 1432-1 Horinouchi, Hachioji, Tokyo 192-0355, Japan*
[d] *Graduate School of Pharmaceutical Sciences, Hokkaido University, Kita-12, Nishi-6, Kita-ku, Sapporo 060-0812, Japan*
[e] *Department of Molecular Neurobiology and Pharmacology, School of Medicine, University of Tokyo, Tokyo 113-0033, Japan*

Received 23 August 2001; accepted 4 September 2001

First published online 18 September 2001

Edited by Maurice Montal

Abstract To develop an assay system that allows the *N*-methyl-D-aspartate (NMDA) receptor subtype-selective antagonistic potency of drugs, we have established Chinese hamster ovary cell lines expressing the four NMDA receptor subtypes (GluRε1/ζ1–GluRε4/ζ1) heat-indelibly. Using these clonal cells, we found that a novel antagonist, (1*S*,2*R*)-1-phenyl-2[(*S*)-1-aminopropyl]-*N*,*N*-diethylcyclopropanecarboxamide, was less selective for the GluRε1/ζ1: the IC_{50} values for the GluRε1/ζ1–GluRε4/ζ1 were 41.7, 13.3, 12.6 and 11.5 μM, respectively, while two well-known antagonists, DL-2-amino-5-phosphonovaleric acid and ifenprodil, showed the known potency and selectivity for each subtype. Thus, the established clonal cells are of use in characterizing the pharmacological properties of drugs that act on NMDA receptors.

Key words: Calcium imaging; Chinese hamster ovary cell; Drug screening; Heat shock promoter; *N*-Methyl-D-aspartate receptor; Subtype selectivity

1. Introduction

The *N*-methyl-D-aspartate (NMDA) subtype of the glutamate receptor (GluR) plays a key role in synaptic plasticity as a molecular coincidence detector [1,2]. Studies using specific antagonists have demonstrated that NMDA receptors play diverse physiological roles in learning, memory and neural development [3]. NMDA receptors are composed of GluRε (NR2) and GluRζ (NR1) subunits [4–6]. The GluRε subunit contains the glutamate binding site, while the GluRζ subunit bears the glycine binding site [7,8]. There are four GluRε subunit genes [4–6,9] and a single GluRζ subunit gene [10,11]. Expression of the four GluRε subunit genes varies depending on brain regions and developmental stages. The four GluRε subunits also differ in terms of functional properties and modulations and are the key determinants of NMDA receptor diversity [12,13]. The physiological significance of the molecular diversity of the NMDA receptor has been examined by gene-targeting techniques. Disruption of the GluRε1 gene results in increased thresholds for hippocampal long-term potentiation and contextual learning [14,15]. GluRε2 mutant mice failed to form the whisker-related neural pattern (barrelettes) in the brainstem trigeminal complex [16], as do GluRζ1 mutant mice [17]. Ablation of the GluRε2 subunit differentially affects plasticity at various hippocampal synapses [16,18]. GluRε4 mutant mice exhibited reduced spontaneous activity [19], while the combination of a GluRε1 and a GluRε3 mutation in mice results in a motor deficit [20,21]. GluRε1 and GluRε4 differentially contributed to pain modulation [22].

Excessive activation of the NMDA receptor may lead to excessive increase in intracellular Ca^{2+} concentration ($[Ca^{2+}]_i$) followed by neurodegeneration [23]. Thus, NMDA receptor antagonists would be useful to protect neurons from brain diseases, such as epilepsy, stroke, ischemia and Parkinson's syndrome [24–26]. However, NMDA receptor antagonists may have various adverse side effects, especially psychotomimetic effects and motor impairment [27,28]. The availability of subtype-selective drugs may minimize the adverse side effects of NMDA receptor antagonists. In fact, the GluRε2 subunit-selective antagonists, CP-101,606 and its derivatives suppress mechanical hyperalgesia and inhibit capsaicin- and 4β-phorbol-12-myristate-12-acetate-induced nociceptive responses without producing any behavioral side effects [29]. It would therefore be useful to develop an assay system of the subtype-selective antagonistic potency of drugs. One approach is to establish recombinant cell lines expressing different subtypes of the NMDA receptor. Previously, we established Chinese hamster ovary (CHO) cell lines that expressed GluRε1/ζ1 NMDA receptors following heat induction [30].

*Corresponding author. Fax: (81)-42-346 1751.
E-mail address: uchino@ncnp.go.jp (S. Uchino).

Abbreviations: CHO, Chinese hamster ovary; $[Ca^{2+}]_i$, intracellular Ca^{2+} concentration; DL-APV, DL-2-amino-5-phosphonovaleric acid; GluR, glutamate receptor; NMDA, *N*-methyl-D-aspartate; PPDC, (1*S*,2*R*)-1-phenyl-2[(*S*)-1-aminopropyl]-*N*,*N*-diethylcyclopropanecarboxamide

PII: S0014-5793(01)02899-X

Here, we extend this approach to the GluRε2/ζ1, GluRε3/ζ1, and GluRε4/ζ1 subtypes of the NMDA receptor.

2. Materials and methods

2.1. Plasmid construction

cDNA fragments containing the entire coding sequences of the GluRζ1 subunit (3.2 kb *Apa*I fragment, nucleotide residues −124–3029), GluRε1 subunit (4.4 kb *Nco*I–*Xba*I fragment, nucleotide residues −66–4329), GluRε2 subunit (4.5 kb *Sal*I–*Bam*HI fragment, nucleotide residues −93–4438), GluRε3 subunit (3.6 kb *Sac*I–*Nco*I fragment, nucleotide residues −156–3801) and GluRε4 subunit (4.2 kb *Sal*I–*Eco*RI fragment, nucleotide residues −81–4078) were prepared. Each fragment was inserted into the *Sal*I site downstream of the *Drosophila* heat shock protein (hsp) 70 promoter in the pHSD mammalian expression vector [30] using blunt-end ligation to yield pHSD-ζ1, pHSD-ε1, pHSD-ε2, pHSD-ε3 and pHSD-ε4.

2.2. Cell culture, DNA transfection and isolation of clonal cells

CHO cells were maintained at 37°C in eRDF-1 medium [30] supplemented with 10% fetal bovine serum (FBS) in a humidified atmosphere containing 5% CO_2.

For transfection, exponentially growing cells were trypsinized, seeded in six-well plates at 2×10^5 cells/well, incubated overnight in eRDF-1 medium supplemented with 10% FBS, then transfected with 15 μg of DNA using the lipopolyamine-mediated procedure, and maintained in selective growth medium [30]. The selective growth media used were eRDF-1 medium containing 10% FBS, 1200 μg/ml of geneticin, 2 μg/ml of blasticidin S hydrochloride, 10 μg/ml of puromycin and 200 μM DL-2-amino-5-phosphonovaleric acid (DL-APV), a specific competitive antagonist of the NMDA receptor added to prevent toxicity due to possible stress-induced leaky expression of NMDA receptors. After about 2 weeks, antibiotic-resistant colonies were picked for expansion and each resistant colony was grown up in two culture dishes. One dish, containing 50–80% confluent cells, was incubated at 43°C for 2 h, then total RNA was immediately extracted to study NMDA receptor mRNA expression, while the other dish was subcultured continuously and tested for functional NMDA receptors by calcium fluorometry. The clonal cells were recloned by limiting dilution.

2.3. Heat induction

CHO cells, plated in selective growth medium at a density of 1.5–2.5×10^4 cells/cm^2 in 100 mm culture dishes for immunoblot experiments and on collagen-coated glass coverslips with a silicon rubber wall (Flexiperm Disc) for calcium imaging, were incubated at 37°C for 24–36 h. They were then incubated at 43°C for 2 h and maintained at 37°C for the indicated periods in the appropriate selective growth medium containing 1 mM DL-APV.

2.4. Immunoblot analysis

CHO cells were lysed in 0.1 M Na_2CO_3 on ice, then pelleted by centrifugation at $18\,000\times g$ for 10 min at 4°C. The pellets were suspended in 50 mM Tris–HCl (pH 7.4), 0.3 mM EDTA, 1 mM dithiothreitol and 1 mM phenylmethanesulfonyl fluoride, then boiled for 5 min with an equal volume of SDS–PAGE sample buffer. The proteins were separated by electrophoresis through a 2–15% gradient SDS polyacrylamide gel (Daiichi Pure Chemicals), then electrophoretically transferred onto polyvinylidene difluoride membranes. To detect the GluRε1, GluRε2, GluRε3 and GluRζ1 subunits, the membranes were blocked by incubation for 2 h at room temperature with 5% dried skimmed milk in phosphate-buffered saline (PBS), then incubated overnight at 4°C with the appropriate primary rabbit antibody (2.0 μg/ml of anti-NMDAR2A, 1.3 μg/ml of anti-NMDAR2B, 2.0 μg/ml of anti-NMDAR2C or 1.0 μg/ml of anti-NMDAR1A; Chemicon), diluted in PBS containing 0.1% Tween (PBS-T). To detect the GluRε4 subunit, the membranes were blocked by incubation for 16 h at 4°C with 5% dried skimmed milk in PBS-T, then incubated for 1 h at room temperature with 3.0 μg/ml of rabbit anti-GluRε4 antibody provided by Dr. K. Sakimura, Niigata University. After rinsing with PBS-T, the blots were incubated with a 1:1000 dilution of horseradish peroxidase-conjugated goat anti-rabbit IgG (Medical and Biological Lab.) and reactive bands visualized using an enhanced chemiluminescence system (Amersham).

2.5. Measurement of $[Ca^{2+}]_i$

CHO cells were plated at a density of $1.5–2.5\times10^4$ cells/cm^2 in selective growth medium on collagen-coated glass coverslips and incubated sequentially at 37°C for 24–36 h and 43°C for 2 h, then maintained at 37°C for the indicated periods before measuring the $[Ca^{2+}]_i$ as described below.

CHO cells were incubated for 45 min with 5.0 μM fura-2 acetoxymethyl ester, dispersed by brief sonication in balanced salt solution (BSS), consisting of 130 mM NaCl, 5.4 mM KCl, 2.0 mM $CaCl_2$, 5.5 mM glucose and 10 mM HEPES (pH 7.3), supplemented with 0.001% cremophore EL (a solubility enhancer). The fura-2-loaded cells were then placed on the stage of an inverted fluorescence microscope (IX50; Olympus) and perfused with BSS at a rate of 2.0 ml/min. Using alternate illumination at 340 and 380 nm excitation, fluorescence images were obtained using a magnification objective lens (UApo 20×/340; Olympus) and an emission filter (510–550 nm), captured using a silicon-intensified-target video camera (C2400-8; Hamamatsu Photonics), digitized using an image processor (Argus 50/CA; Hamamatsu Photonics) and the data fed into a personal computer (Venturis FXs, Digital). For ratiometry, ratio images were obtained by dividing the fluorescence intensity at 340 nm excitation (F_{340}) by that at 380 nm excitation (F_{380}) using the computer and the image processor. The cytosolic free Ca^{2+} concentration was estimated from a calibration curve of fura-2 fluorescence ratio (F_{340}/F_{380}) versus Ca^{2+} concentration, established using dilutions of a Ca^{2+} solution of known concentration (Calcium Calibration Buffer kit with Magnesium I; Molecular Probes) containing 30 μM fura-2 free acid and the same optical settings as those used for the CHO cells.

2.6. Data analysis

Concentration–inhibition curves were fitted by the logistic equation:

$$I/I_{\text{control}} = 1/\{1 + ([\text{antagonist}]/\text{IC}_{50})^n\},$$

where I_{control} is the response in the absence of the antagonist, IC_{50} is the concentration of the drug that inhibits 50% of this response and n is the Hill coefficient.

IC_{50} values for DL-APV were corrected for L-glutamate affinity according to the equation:

$$\text{IC}_{50} = \text{IC}_{50}{}^*/\{1 + ([\text{L} - \text{glutamate}]/\text{EC}_{50})\},$$

where IC_{50}* is the measured value obtained from the inhibition curve, [L-glutamate] is 100 μM and the EC_{50} values for L-glutamate are 1.7, 0.8, 0.7, and 0.4 μM for the GluRε1/ζ1, GluRε2/ζ1, GluRε3/ζ1, and GluRε4/ζ1 subtypes, respectively [13].

3. Results

3.1. Establishment of CHO cell lines expressing NMDA receptor subtypes upon heat induction

We placed the respective GluRε subunit cDNAs under the control of *Drosophila* hsp70 gene promoter in the pHSD expression vector. To establish a cell line expressing the GluRε2/ζ1 subtype, plasmids pHSD-ε2 and pSV2*brs* carrying the blasticidin S hydrochloride resistance gene were co-transfected into Z1-1 CHO cells carrying the heat-inducible GluRζ1 expression vector pHSD-ζ1 [30]. Resulting geneticin- and blasticidin S hydrochloride-resistant clones were screened for the heat-inducible expression of GluRε2 mRNA by RNA blot hybridization analysis. Further screening for functional NMDA receptor expression by measuring 100 μM L-glutamate plus 100 μM glycine-inducible $[Ca^{2+}]_i$ responses established cell line ZE2-1. Further transfection of ZE2-1 cells with pHSD-ζ1 and pSV2*pur* carrying the puromycin resistance gene yielded E2 cell line, which expressed high levels of GluRε2/ζ1 subtype NMDA receptors following heat induction. The E1 cell line expressing a high level of the GluRε1/ζ1 subtype was produced similarly by transfection of ZE1-1 cells with pHSD-ζ1.

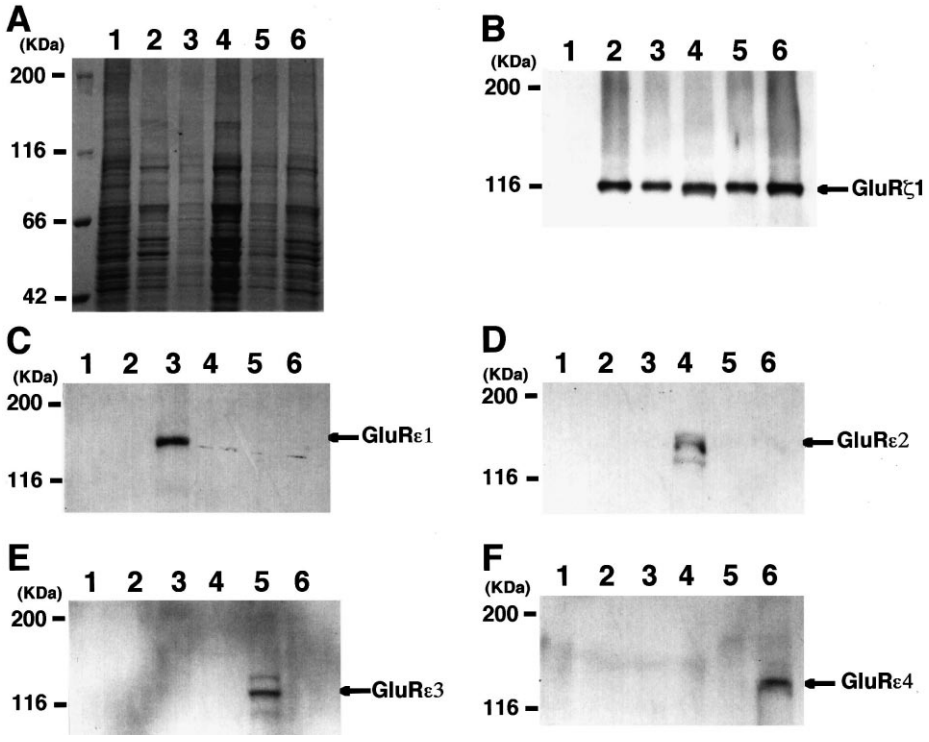

Fig. 1. Heat-inducible expression of GluRζ1, GluRε1, GluRε2, GluRε3, and GluRε4 subunits in clonal cells. Proteins were separated by electrophoresis through a 2–15% gradient SDS polyacrylamide gel and stained with Coomassie brilliant blue (A). Molecular weight standards (42–200 kDa; Daiichi Pure Chemicals) are indicated on the left. The separated proteins were transferred and detected using NMDAR1A (B), NMDAR2A (C), NMDAR2B (D), NMDAR2C (E) or GluRε4 (F) antibodies. Lane 1: sample prepared from 1.5×10^6 CHO cells; lane 2: sample prepared from 3.6×10^5 Z1 cells; lane 3: sample prepared from 3.6×10^5 E1 cells; lane 4: sample prepared from 1.5×10^6 E2 cells; lane 5: sample prepared from 7.2×10^5 E3 cells; lane 6: sample prepared from 7.2×10^5 E4 cells. The expected molecular weight for each subunit is indicated on the right.

To establish cell lines expressing the GluRε3/ζ1 and GluRε4/ζ1 subtypes, we first isolated the Z1 cell line by co-transfecting CHO cells with pHSD-ζ1 and pSV2*neo*. RNA blot hybridization showed that Z1 cells expressed more GluRζ1 mRNA than the previously produced Z1-1 cells (data not shown). Z1 cells were then transfected with pHSD-ε3 or pHSD-ε4 expression vector. Screening of resulting clones established E3 and E4 cell lines, which, respectively, produced high levels of the GluRε3/ζ1 and GluRε4/ζ1 subtypes following heat induction.

The growth rates and shapes of the heat-induced and non-heat-induced cells were indistinguishable. The inducible expression of functional NMDA receptors in an established cell line was stable for at least 25 passages.

3.2. Heat-inducible expression of NMDA receptor subtypes

To study the heat-inducible expression of subunit proteins, membrane fractions were prepared from cells cultured for 6 h after heat induction. Fig. 1 shows immunoblot analyses of the subunits produced in the cell lines. The molecular masses of the GluRζ1 (115 kDa; Fig. 1B), GluRε1 (170 kDa; Fig. 1C), GluRε2 (170 kDa; Fig. 1D), GluRε3 (130 kDa; Fig. 1E) and GluRε4 (140 kDa; Fig. 1F) subunits are in good agreement with those determined for the respective subunits in mouse

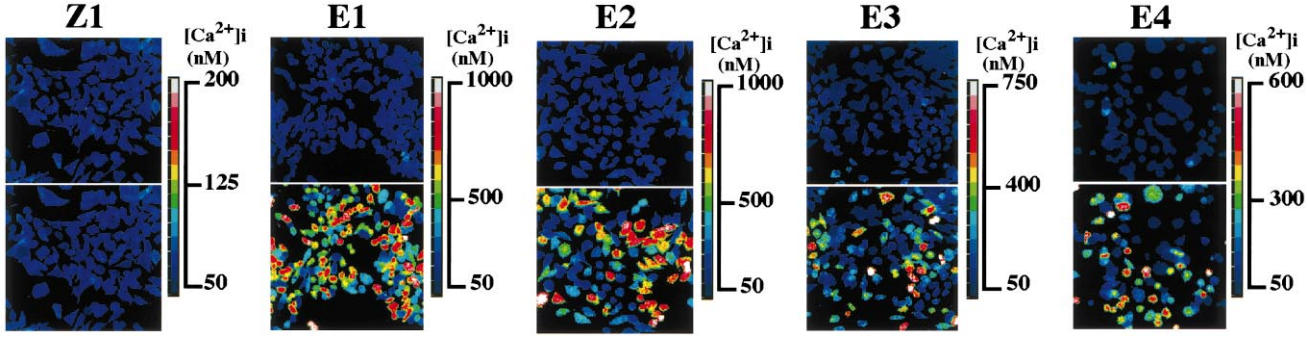

Fig. 2. $[Ca^{2+}]_i$ responses to L-glutamate plus glycine in clonal cells. After heat induction, Z1, E1 and E2 cells were incubated for 6 h at 37°C, while E3 and E4 cells were incubated for 10 h at 37°C. The upper (−Glu/Gly) and lower (+Glu/Gly) panels show images of the cells before and after 100 μM L-glutamate plus 100 μM glycine application, respectively. The corresponding values of the $[Ca^{2+}]_i$ are given by the color scale on the right.

brain. No subunit proteins were detectable in non-induced cells or control CHO cells.

We examined the expression of functional NMDA receptors by measuring the $[Ca^{2+}]_i$ increase in response to 100 μM L-glutamate plus 100 μM glycine. As shown in Fig. 2, the E1, E2, E3 and E4 cell lines, but not Z1 cells, showed clear $[Ca^{2+}]_i$ responses 6–10 h after heat induction. Virtually no responses were seen in Ca^{2+}-free BSS (data not shown), indicating that the $[Ca^{2+}]_i$ increase was due to the Ca^{2+} influx into the cells. No responses were detectable in the absence of heat induction (data not shown).

3.3. Sensitivity to DL-APV and ifenprodil of NMDA receptor subtypes expressed in CHO cell lines

The heat-induced cells showed reproducible $[Ca^{2+}]_i$ responses to repeated applications of 100 μM L-glutamate plus 100 μM glycine (applications for 30 s with an interval of 15 min) (Fig. 3). Thus, the expressed NMDA receptors showed little desensitization under these experimental conditions. Using these clonal cell lines and calcium fluorometry, we investigated the antagonistic potency and subtype selectivity of the typical antagonists, DL-APV and ifenprodil. We first measured the $[Ca^{2+}]_i$ response to 100 μM L-glutamate plus 100 μM glycine for 30 s. After washing with BSS for 15 min, we applied antagonist for 30 s, antagonist and L-glutamate plus glycine for 30 s, and then antagonist for 30 s successively. After washing with BSS for 15 min, we applied L-glutamate plus glycine for 30 s to examine the recovery of the response.

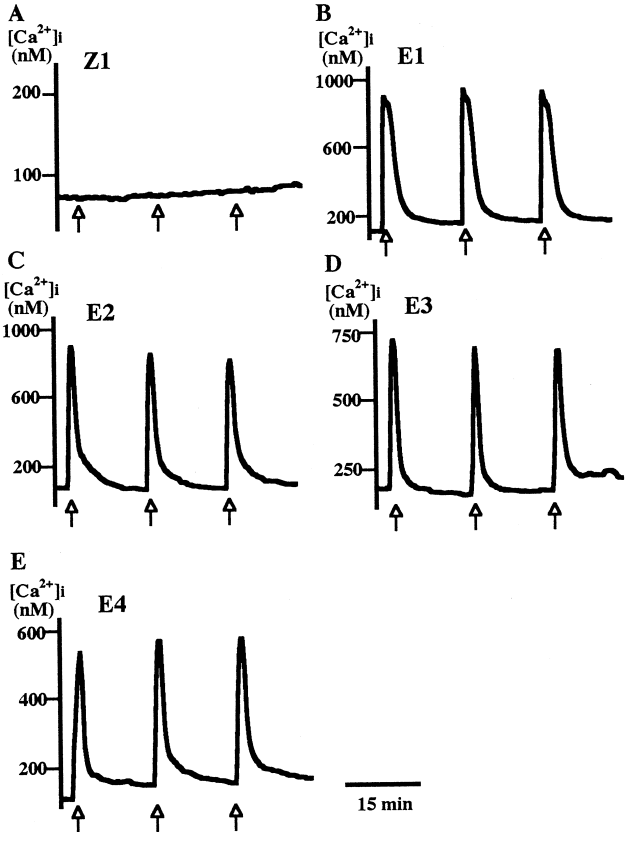

Fig. 3. $[Ca^{2+}]_i$ responses of clonal cells to three successive applications of L-glutamate plus glycine. Kinetic traces for the evoked Ca^{2+} signals are shown for Z1 cells (A), E1 cells (B), E2 cells (C), E3 cells (D) and E4 cells (E). After heat induction, the Z1, E1 and E2 cells were incubated for 6 h at 37°C, while the E3 and E4 cells were incubated for 10 h. The 30 s applications of 100 μM L-glutamate plus 100 μM glycine are indicated by arrows. The data are the mean values for seven individual cells.

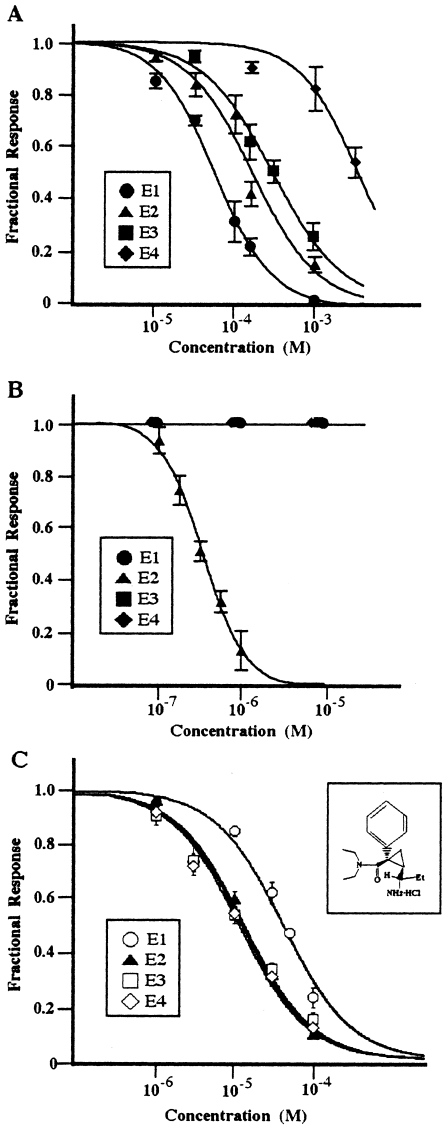

Fig. 4. Inhibitory effects of DL-APV (A), ifenprodil (B) and PPDC (C) on the $[Ca^{2+}]_i$ responses to 100 μM L-glutamate plus 100 μM glycine (A, B) or 30 μM L-glutamate plus 30 μM glycine (C). After heat induction, the cells were incubated for 6–10 h at 37°C. Data were done in triplicate and shown as mean ± S.D. The structure of PPDC is shown in the insert.

DL-APV inhibited the responses of all four cell lines with varying efficiency (Fig. 4A). Since the four NMDA receptor subtypes have different affinities for L-glutamate [19], the IC_{50} values obtained from inhibition curves were corrected for L-glutamate affinity in order to examine the subtype sensitivity [31]. The corrected IC_{50} values of DL-APV for the GluRε1/ζ1, GluRε2/ζ1, GluRε3/ζ1 and GluRε4/ζ1 subtypes were 0.88 ± 0.03 μM ($n = 3$), 1.45 ± 0.10 μM ($n = 3$), 2.39 ± 0.03 μM ($n = 3$) and 17.5 ± 1.5 μM ($n = 3$), respectively. The Hill coefficient values for the GluRε1/ζ1, GluRε2/ζ1, GluRε3/ζ1 and GluRε4/ζ1 subtypes were 1.2 ± 0.04, 1.0 ± 0.1, 1.2 ± 0.1 and 0.8 ± 0.03, respectively. The rank order of sensitivity to DL-APV was GluRε1/ζ1 > GluRε2/ζ1 > GluRε3/ζ1 > GluRε4/

ζ1 subtypes, in accordance with the previous studies by the *Xenopus* oocyte expression system [13,31].

Ifenprodil is a GluRε2/ζ1 subtype-selective antagonist acting at the polyamine modulatory site [32]. As expected, the GluRε2/ζ1 subtype was highly sensitive to ifenprodil (IC_{50}: 0.35 ± 0.03 μM, Hill coefficient: 2.0 ± 0.2, $n = 3$), whereas concentrations greater than 100 μM were required to affect the responses of E1, E3 and E4 cells (Fig. 4B).

3.4. Characterization of the subtype selectivity of a novel NMDA antagonist using the cell lines

(1*S*,2*R*)-1-Phenyl-2[(*S*)-1-aminopropyl]-*N*,*N*-diethylcyclopropanecarboxamide (PPDC) is a novel non-competitive NMDA receptor antagonist [33]. We investigated the antagonistic potency and subtype selectivity of PPDC using the established CHO cell lines. The inhibitory effects of PPDC on the $[Ca^{2+}]_i$ responses of the cell lines to 30 μM L-glutamate plus 30 μM glycine are shown in Fig. 4C. The IC_{50} values of PPDC for the GluRε1/ζ1, GluRε2/ζ1, GluRε3/ζ1 and GluRε4/ζ1 subtypes were 41.7 ± 1.5 μM (Hill coefficient: 0.9 ± 0.1, $n = 3$), 13.3 ± 0.5 μM (1.1 ± 0.1, $n = 3$), 12.6 ± 0.5 μM (1.0 ± 0.1, $n = 3$) and 11.5 ± 1.2 μM (1.0 ± 0.1, $n = 3$), respectively. The effect of PPDC was essentially reversible and lost after a 15 min washing.

4. Discussion

Extensive studies have been performed to characterize the properties and selectivity of various NMDA receptor ligands using brain slices and cultured neurons [34,35]. Because of possible heterogeneity in terms of cell type and receptor subtype, such studies are of limited use in the precise determination of the characterization and subtype specificity of NMDA receptor ligands. The four GluRε subunits carrying the glutamate binding site of the NMDA receptor are distinct in terms of distribution, functional properties and modulation. Transient expression of NMDA receptors in *Xenopus* oocytes [13,31] and HEK293 cells [6,36,37] has been used to examine their pharmacological properties. However, these approaches are less convenient and reproducible for drug assays on a regular basis than a permanent expression system, such as a stably transfected cell line. Thus, the availability of recombinant cells expressing these subtypes of the NMDA receptor would be useful in their characterization and in the development of subtype-selective drugs. Constitutive expression of exogenous NMDA receptors, however, is toxic to host cells [38,39]. In previous studies, a dexamethasone-inducible promoter [40–42] and a tetracycline sensitive transactivator system [43] were used to express the GluRε1/ζ1 and GluRε2/ζ1 subtypes. In the present study, we used an expression vector containing the inducible *Drosophila* hsp70 promoter to express NMDA receptors in CHO cells. Using this approach, we have successfully established clonal CHO cell lines expressing respective subtypes of the NMDA receptor upon heat induction.

After heat induction, we observed a significant increase in the L-glutamate plus glycine-evoked $[Ca^{2+}]_i$ response in more than 80% of E1 cells and about 50% of E2, E3 and E4 cells. This result, together with those of the Western blot analyses in which the strongest signal was seen with E1 cells, shows that E1 cells produce a higher level of functional NMDA receptors compared with the other clonal cells. In order to increase the percentage of cells expressing functional NMDA receptors and the expression level of functional NMDA receptors, recloning by limiting dilution and/or re-introduction of subunit cDNAs into E2, E3 or E4 cells would probably be useful approaches. Interestingly, despite the fact that expression of subunit proteins was lower in E2 cells than in E3 or E4 cells, the peak of the L-glutamate plus glycine-induced response in E2 cells was higher than in E3 or E4 cells, and almost as high as in E1 cells. This result was in agreement with that of Northern blot analysis in which the weakest signal was seen with E2 cells (data not shown). One explanation for this discrepancy would be the difference in Ca^{2+} permeability between NMDA receptor subtypes. The Ca^{2+}/Cs^{+} permeability ratio is lower for GluRε3/ζ1 than for GluRε1/ζ1 [37], while GluRε1/ζ1 and GluRε2/ζ1 have similar Ca^{2+} permeability [44]. In addition, functional expression of similar amounts of GluRε1/ζ1 or GluRε2/ζ1, but not GluRε3/ζ1, resulted in cell death, and the authors suggested that this difference in vulnerability was due to differences in Ca^{2+} permeability between the NMDA receptor subtypes [39].

Whole cell recording and binding assays have been conventionally used to characterize drugs. However, whole cell recording is not amenable to a high throughput. Binding assays require relatively large amounts of purified receptor-containing membranes, are restricted by the availability of suitable radioactive ligands, and are not functional assays. In contrast, the digital calcium imaging technique can be easily used for functional analysis of receptors, and advanced machinery for this technique has recently been developed, allowing high throughput. Moreover, in HEK293 cells, the IC_{50} value for toxicity is reported to be closer to the IC_{50} value measured by calcium fluorometry than to that measured by ligand binding experiments [45]. In the present study, we therefore employed the digital calcium imaging technique using the dye fura-2, in a model study of the effects on the four NMDA receptor subtypes of two well-characterized NMDA receptor antagonists, DL-APV and ifenprodil, and a novel antagonist, PPDC.

Since three successive administrations of agonists were found to induce comparable responses, it was possible to study antagonistic potency and reversibility of effects in a precise manner. The four NMDA receptor subtypes showed differential sensitivity to DL-APV. The corrected IC_{50} values of DL-APV were 0.88 ± 0.03 μM for GluRε1/ζ1, 1.45 ± 0.10 μM for GluRε2/ζ1, 2.39 ± 0.03 μM for GluRε3/ζ1, 17.5 ± 1.48 μM for GluRε4/ζ1. The observed rank order is in accordance with that found in the *Xenopus* oocytes expression system [13,31]. The present study shows that the antagonistic effect of ifenprodil was highly selective for GluRε2/ζ1, and the IC_{50} value (0.35 ± 0.03 μM) was close to that obtained using GluRε2/ζ1 expressed in *Xenopus* oocytes (0.34 μM) [32]. These results indicate that our system works properly in determining the potency and selectivity of drugs.

In the present study, we also determined the sensitivity of NMDA receptor subtypes to PPDC. PPDC is a conformationally restricted analog of milnacipran [33]. Although milnacipran, a potent inhibitor of serotonin (5HT) uptake, suppresses the binding of MK-801 to NMDA receptors [46], its structure is quite different from that of MK-801. Recent studies have shown that PPDC decreases the maximal responses to both NMDA and glycine without altering their dissociation constants. It has no effects on the other GluR families (AMPA, kainate and metabotropic GluRs) or on other neuro-

transmitter receptors (GABAA, 5HT2C and acetylcholine receptors) [47]. Thus, PPDC is a specific and non-competitive antagonist for NMDA receptors. The present study shows that PPDC had less effect on the GluRε1/ζ1 subtype than on other subtypes. Since stable cell lines and digital calcium imaging technique will facilitate a rapid functional high throughput assay, these CHO cell lines will provide a useful tool for the development of NMDA receptor subtype-selective drugs.

Acknowledgements: We thank Dr. Kenji Sakimura for his kind gift of rabbit anti-GluRε4 antibody and Mariko Shiomi for her technical assistance. This study was supported by NEDO (New Energy and Industrial Technology Development Organization) as a R&D project of the Industrial Science and Technology Frontier Program and by the Program for Promotion of Fundamental Studies in Health Science of the Organization for Drug ADR Relief, R&D Promotion and Product Review of Japan.

References

[1] Bliss, T.V.P. and Collingridge, G.L. (1993) Nature 361, 31–39.
[2] Malenka, R.C. and Nicoll, R.A. (1993) Trends Neurosci. 16, 521–527.
[3] Morris, R.G., Anderson, E., Lynch, G.S. and Baudry, M. (1986) Nature 319, 774–776.
[4] Kutsuwada, T., Kashiwabuchi, N., Mori, H., Sakimura, K., Kushiya, E., Araki, K., Meguro, H., Masaki, H., Kumanishi, T., Arakawa, M. and Mishina, M. (1992) Nature 358, 36–41.
[5] Meguro, H., Mori, H., Araki, K., Kushiya, E., Kutsuwada, T., Yamazaki, M., Kumanishi, T., Arakawa, M., Sakimura, K. and Mishina, M. (1992) Nature 357, 70–74.
[6] Monyer, H., Sprengel, R., Schoepfer, R., Herb, A., Higuchi, M., Lomeli, H., Burnashev, N., Sakmann, B. and Seeburg, P.H. (1992) Science 256, 1217–1221.
[7] Kuryatov, A., Laube, B., Betz, H. and Kuhse, J. (1994) Neuron 12, 1291–1300.
[8] Uchino, S., Nakajima-Iijima, S., Okuda, K., Mishina, M. and Kawamoto, S. (1997) NeuroReport 8, 445–449.
[9] Ikeda, K., Nagasawa, M., Mori, H., Araki, K., Sakimura, K., Watanabe, M., Inoue, I. and Mishina, M. (1992) FEBS Lett. 313, 34–38.
[10] Moriyoshi, K., Masu, M., Ishii, T., Shigemoto, R., Mizuno, N. and Nakanishi, S. (1991) Nature 354, 31–37.
[11] Yamazaki, M., Mori, H., Araki, K., Mori, K.J. and Mishina, M. (1992) FEBS Lett. 300, 39–45.
[12] Seeburg, P.H. (1993) Trends Neurosci. 16, 359–365.
[13] Mori, H. and Mishina, M. (1995) Neuropharmacology 34, 1219–1237.
[14] Sakimura, K., Kutsuwada, T., Ito, I., Manabe, T., Takayama, C., Kushiya, E., Yagi, T., Aizawa, S., Inoue, Y., Sugiyama, H. and Mishina, M. (1995) Nature 373, 151–155.
[15] Kiyama, Y., Manabe, T., Sakimura, K., Kawakami, F., Mori, H. and Mishina, M. (1998) J. Neurosci. 18, 6704–6712.
[16] Kutsuwada, T., Sakimura, K., Manabe, T., Takayama, C., Katakura, N., Kushiya, E., Natsume, R., Watanabe, M., Inoue, Y., Yagi, T., Aizawa, S., Arakawa, M., Takahashi, T., Nakamura, Y., Mori, H. and Mishina, M. (1996) Neuron 16, 333–344.
[17] Li, Y., Erzurumlu, R.S., Chen, C., Jhaveri, S. and Tonegawa, S. (1994) Cell 76, 427–437.
[18] Ito, I., Futani, K., Katagiri, H., Watanabe, M., Sakimura, K., Mishina, M. and Sugiyama, H. (1997) J. Physiol. 500, 401–408.
[19] Ikeda, K., Araki, K., Takayama, C., Inoue, Y., Yagi, T., Aizawa, S. and Mishina, M. (1995) Mol. Brain Res. 33, 61–71.
[20] Ebralidze, A.K., Rossi, D.J., Tonegawa, S. and Slater, N.T. (1996) J. Neurosci. 16, 5014–5025.
[21] Kadotani, H., Hirano, T., Masugi, M., Nakamura, K., Nakao, K., Katsuki, M. and Nakanishi, S. (1996) J. Neurosci. 16, 7859–7867.
[22] Mitani, T., Okuda-Ashitaka, E., Hori, Y., Sakuma, S., Sugimoto, T., Sakimura, K., Mishina, M. and Ito, S. (1999) Eur. J. Neurosci. 11, 1849–1856.
[23] Choi, D.W. (1988) Neuron 1, 623–634.
[24] Dingledine, R., McBain, C.J. and McNamara, J.O. (1990) Trends Pharmacol. Sci. 11, 334–338.
[25] McCulloch, J. (1992) Br. J. Clin. Pharmacol. 34, 106–114.
[26] Lipton, S.A. (1993) Trends Neurosci. 16, 527–532.
[27] Willetts, J., Balster, R.D. and Leander, J.D. (1990) Trends Pharmacol. Sci. 11, 423–428.
[28] Rogawski, M.A. (1993) Trends Pharmacol. Sci. 14, 325–331.
[29] Taniguchi, K., Shinjo, K., Mizutani, M., Shimada, K., Ishikawa, T., Menniti, F.S. and Nagahisa, A. (1997) Br. J. Pharmacol. 122, 809–812.
[30] Uchino, S., Kudo, Y., Watanabe, W., Nakajima-Iijima, S. and Mishina, M. (1997) Mol. Brain Res. 44, 1–11.
[31] Buller, A.L. and Monaghan, D.T. (1997) Eur. J. Pharmacol. 320, 87–94.
[32] Williams, K. (1993) Mol. Pharmacol. 44, 851–859.
[33] Shuto, S., Ono, S., Hase, Y., Noguchi, T., Yoshii, K. and Matsuda, A. (1996) J. Med. Chem. 39, 4844–4852.
[34] Rothman, S.M., Thurston, J.H. and Hauhart, R.E. (1987) Neuroscience 22, 472–480.
[35] Garthwaite, G. and Garthwait, J. (1989) Neurosci. Lett. 97, 316–322.
[36] Monyer, H., Burnashev, N., Laurie, D.J., Sakmann, B. and Seeburg, P.H. (1994) Neuron 12, 529–540.
[37] Burnashev, N., Zhou, Z., Neher, E. and Sakmann, B. (1995) J. Physiol. 485, 403–418.
[38] Anegawa, N.J., Lynch, D.R., Verdoorn, T.A. and Pritchett, D.B. (1995) J. Neurochem. 64, 2004–2012.
[39] Boeckman, F.A. and Aizenman, E. (1996) J. Pharmacol. Exp. Ther. 279, 515–523.
[40] Priestley, T., Laughton, P., Myers, J., Le Bourdelles, B., Kerby, J. and Whiting, P.J. (1995) Mol. Pharmacol. 48, 841–848.
[41] Grimwood, S., Le Bourdelles, B., Atack, J.R., Barton, C., Cockett, W., Cook, S.M., Gilbert, E., Hutson, P.H., McKernan, R.M., Myers, J., Ragan, C.I., Wingrove, P.B. and Whiting, P.J. (1996) J. Neurochem. 66, 2239–2247.
[42] Varney, M.A., Jachec, C., Deal, C., Hess, S.D., Daggett, L.P., Skvoretz, R., Urcan, M., Morrison, J.H., Moran, T., Johnson, E.C. and Veligelebi, G. (1996) J. Pharmacol. Exp. Ther. 279, 367–378.
[43] Renard, S., Drouet-Petre, C., Partiseti, M., Langer, S.L., Graham, D. and Besnard, F. (1999) Eur. J. Pharmacol. 366, 319–328.
[44] Grimwood, S., Gilbert, E., Ragan, C.I. and Hutson, P.H. (1996) J. Neurochem. 66, 2589–2595.
[45] Grant, E.R., Bacskai, B.J., Pleasure, D.E., Pritchett, D.B., Gallagher, M.J., Kendrick, S.J., Kricka, L.J. and Lynch, D.R. (1997) J. Cell Biol. 272, 647–656.
[46] Shuto, S., Takada, H., Mochizuki, D., Tsujita, R., Hase, Y., Ono, S., Shibuya, N. and Matsuda, A. (1995) J. Med. Chem. 38, 2964–2968.
[47] Noguchi, T., Ishii, K., Ohtsubo, Y., Shuto, S., Ono, S., Matsuda, A. and Yoshii, K. (1999) Synapse 31, 87–96.